IEEE Access
Multidisciplinary | Rapid Review | Open Access Journal

Received November 8, 2019, accepted January 1, 2020, date of publication January 6, 2020, date of current version January 15, 2020.

Digital Object Identifier 10.1109/ACCESS.2020.2964096

Expedited Design Closure of Antenna Input Characteristics by Trust Region Gradient Search and Principal Component Analysis

JON ATLI TOMASSON[1], SLAWOMIR KOZIEL[1,2], (Senior Member, IEEE), AND ANNA PIETRENKO-DABROWSKA[2], (Member, IEEE)

[1]Engineering Optimization and Modeling Center, Department of Technology, Reykjavik University, 101 Reykjavik, Iceland
[2]Faculty of Electronics, Telecommunications and Informatics, Gdansk University of Technology, 80-233 Gdansk, Poland

Corresponding author: Slawomir Koziel (koziel@ru.is)

This work was supported in part by the Icelandic Centre for Research (RANNIS) Grant 174114051, and in part by the National Science Centre of Poland Grant 2015/17/B/ST6/01857.

ABSTRACT Optimization-based parameter tuning has become an inherent part of contemporary antenna design process. For the sake of reliability, it is typically conducted at the level of full-wave electromagnetic (EM) simulation models. This may incur considerable computational expenses depending on the cost of an individual EM analysis, the number of adjustable variables, the type of task (local, global, single-/multi-objective optimization), and the constraints involved. For these reasons, utilization of conventional algorithms is often impractical. This paper proposes a novel gradient-based algorithm with numerical derivatives for expedited antenna optimization. The improvement of computational efficiency is obtained by employing a rank-one Broyden formula and restricting finite differentiation sensitivity updates to the principal directions of the Jacobian matrix, i.e., those corresponding to the most significant changes of the antenna responses. Comprehensive numerical validation carried out using three wideband antennas indicates that the presented methodology offers considerable savings of sixty percent with respect to the reference trust-region algorithm. At the same time, virtually no degradation of the design quality is observed. Furthermore, algorithm reliability is greatly improved (while offering comparable computational efficiency) over the recent state-of-the-art accelerated gradient-based procedures.

INDEX TERMS Antenna design, design closure, gradient-based optimization, principal component analysis, electromagnetic (EM) simulation.

I. INTRODUCTION

Design of modern antenna structures is a complex process. Among several stages involved, the final adjustment of geometry parameters (also referred to as design closure) plays an increasingly important role [1]–[4]. Although the tuning process is still predominantly conducted using experience-driven parameter sweeping, automated adjustment through rigorous numerical optimization is becoming more and more widespread [5], [6]. The principal reasons include the necessity of handling multiple and often conflicting objectives pertaining to both electrical and field characteristics of the antenna at hand (e.g., impedance matching, gain, axial ratio, radiation pattern) [7], [8], satisfying various constraints (e.g., imposed on antenna size [9], [10]), as well as operating in highly-dimensional parameter spaces. For the sake of reliability, carrying out the design closure at the level of full-wave electromagnetic (EM) simulation models is essentially imperative, as simpler representations (analytical, equivalent network) are either unavailable or grossly inaccurate. In particular, EM analysis is the only versatile tool that permits accounting for mutual radiator coupling [11], the effects of connectors and housing [12], feed radiation, or quantifying complex interactions of geometry parameters responsible for exciting orthogonal modes in circular polarization antennas [13].

The primary bottleneck of EM-driven design closure is its high computational cost. Even local optimization (both gradient-based [14] and derivative-free [15]) typically involves dozens or hundreds of EM analyses. Whereas global

The associate editor coordinating the review of this manuscript and approving it for publication was Lin Peng.

search using population-based metaheuristics (evolutionary algorithms [16], particle swarm optimizers [17], differential evolution [18], harmony search [19]) or uncertainty quantification (statistical analysis [20], robust design [21]) require significantly larger amounts of objective function evaluations. The cost of these procedures may be prohibitive. It is not surprising that significant research efforts have been focused on the development of optimization procedures featuring improved computational efficiency. These include incorporation of adjoint sensitivities into gradient-based algorithms [22], [23], which is a very attractive concept; however, the adjoint technology is only supported by a few commercial solvers (e.g., [24]). Surrogate-based optimization (SBO) is another class of methods of growing popularity [25], [26]. The keystone of SBO is shifting the computational burden into a fast replacement model (surrogate), while referring to an original (high-fidelity) EM model only occasionally, for design verification and updating the surrogate. Surrogate-assisted techniques may involve data-driven models (kriging [27], Gaussian process regression [28]) or physics-based ones (space mapping [29], response correction methods [30], adaptive response scaling [31], feature-based optimization [32]). In the context of global search, efficient global optimizers involving combination of approximation surrogates and adaptive sampling techniques [33] are often employed.

Assuming the availability of a decent initial design—often a result of parameter sweeping conducted at the early stages of antenna development—local optimization is normally sufficient. A prerequisite for speeding up local search algorithms, including direct EM-driven design and variable-fidelity SBO techniques [34], is a reduction of the number of antenna simulations at any relevant level of fidelity. Towards this end, several variations of the trust-region (TR) gradient search procedures have been recently proposed [35]–[37]. The principal idea is the omission of finite-differentiation (FD) sensitivity updates for certain variables under specific circumstances. In [35], the criterion was small design relocation in particular directions, whereas in [36], suppression of FD was made dependent on a sufficient alignment between the design relocation direction and coordinate system basis vectors. The method of [37] was based on monitoring variability of antenna response gradients. The aforementioned algorithms offer significant speedup of up to sixty percent with respect to the reference TR procedure. Unfortunately, the improvement of computational efficiency is achieved at the expense of visible design quality degradation.

This paper proposes an alternative implementation of the expedited gradient-based procedure. Our methodology is based on detecting the most important directions in the parameter space, according to their effects on the antenna characteristics, and restricting the FD sensitivity updates to the respective subspaces. Quantification of the direction importance (averaged over the assumed frequency sweep) is realized using the principal component analysis (PCA) [38]; here, the antenna response gradients are treated as observables the correlation of which are determined through PCA. The FD updates applied along the principal components are supplemented by the Broyden formula executed for the candidate designs rendered by the optimization algorithm. The presented approach has been validated using three examples of miniaturized wideband monopole antennas and benchmarked against the reference TR procedure and the accelerated versions of [35]–[37]. The results indicate that our methodology permits sixty percent speedup over the reference algorithm and the efficiency comparable with [35]–[37]. At the same time, no quality degradation has been observed, which was the fundamental issue for the methods reported so far.

II. EXPEDITED OPTIMIZATION USING TRUST-REGION GRADIENT SEARCH AND PRINCIPAL COMPONENTS

This section formulates the antenna design closure task and recalls the reference algorithm being the foundation of the expedited procedure introduced in the work. Subsequently, the proposed use of principal component analysis is discussed in detail, and the flow of the algorithm incorporating principal components as the key accelerating factor is displayed. A comparison is made with recently reported Jacobian updating schemes.

A. ANTENNA DESIGN AS AN OPTIMIZATION TASK

Consider a vector $\boldsymbol{x} = [x_1 \ldots x_n]^T$, where x_i represents the ith geometry parameter of the antenna structure at hand. A goal of the design closure task is the adjustment of $\boldsymbol{x}$, whilst usually retaining a fixed antenna topology, so that the performance figures of choice are improved as much as possible. The task can be described as a nonlinear minimization in the form

$$\boldsymbol{x}^* = \arg\min_{\boldsymbol{x}} U(\boldsymbol{R}(\boldsymbol{x})) \tag{1}$$

where $\boldsymbol{x}^*$ denotes the optimal solution, i.e., the minimizer of the scalar merit function $U(\boldsymbol{R}(\boldsymbol{x}))$ with $\boldsymbol{R}(\boldsymbol{x})$ representing the relevant antenna characteristics evaluated through EM analysis. Clearly, the particular formulation of U is problem-dependent. In the numerical experiments carried out in Section III, minimization of the in-band reflection is considered with the minimax merit function defined as

$$U(\boldsymbol{R}(\boldsymbol{x})) = \max_{f \in F} |S_{11}(\boldsymbol{x}, f)| \tag{2}$$

where F denotes the operating frequency band.

B. REFERENCE ALGORITHM

Here, an outline of the trust-region (TR) gradient search procedure with numerical derivatives (e.g., [14]) is provided. In this work, it is utilized as a reference algorithm. The procedure yields a series $\boldsymbol{x}^{(i)}$, $i = 0, 1, \ldots$, of approximations to the optimum design $\boldsymbol{x}^*$, generated as described below. Let

$$\boldsymbol{L}^{(i)}(\boldsymbol{x}) = \boldsymbol{R}(\boldsymbol{x}^{(i)}) + \boldsymbol{J}_R(\boldsymbol{x}^{(i)}) \cdot (\boldsymbol{x} - \boldsymbol{x}^{(i)}) \tag{3}$$

be a first-order Taylor expansion of $\boldsymbol{R}$ at $\boldsymbol{x}^{(i)}$, where

$$\boldsymbol{J}_R = \begin{bmatrix} \nabla_1^T(\boldsymbol{x}) \\ \vdots \\ \nabla_m^T(\boldsymbol{x}) \end{bmatrix} = \begin{bmatrix} \frac{\partial R_1}{\partial x_1} & \cdots & \frac{\partial R_1}{\partial x_n} \\ \vdots & \ddots & \vdots \\ \frac{\partial R_m}{\partial x_1} & \cdots & \frac{\partial R_m}{\partial x_n} \end{bmatrix} \tag{4}$$

is the Jacobian matrix, representing sensitivities of the antenna outputs $\boldsymbol{R}$. Here, R_k stands for the kth response component, in practice, evaluation of a particular antenna characteristic at the kth discrete frequency within the frequency band of interest. Unless adjoint sensitivities are available, $\boldsymbol{J}_R$ is estimated through finite differentiation. Given the current design $\boldsymbol{x}^{(i)}$, the linear model serves to produce the next approximation, $\boldsymbol{x}^{(i+1)}$ via proxy of the optimum solution $\boldsymbol{x}^*$ at iteration $i = 0, 1, \ldots$

$$\boldsymbol{x}^{(i+1)} = \arg \min_{\boldsymbol{x};\ -\boldsymbol{d}^{(i)} \le \boldsymbol{x} - \boldsymbol{x}^{(i)} \le \boldsymbol{d}^{(i)}} U(\boldsymbol{L}^{(i)}(\boldsymbol{x})) \tag{5}$$

The search process in (5) is bound by a trust region of the size $\boldsymbol{d}^{(i)}$, so that $\boldsymbol{x}^{(i)} - \boldsymbol{d}^{(i)} \le \boldsymbol{x} \le \boldsymbol{x}^{(i)} + \boldsymbol{d}^{(i)}$. The inequality is understood component-wise to accommodate the variability in geometric parameter ranges. The result is a hypercubic search perimeter updated based on gain ratio ρ [39], defined as the ratio of actual versus linear-model-predicted improvement of the merit function.

$$\rho = \frac{U(\boldsymbol{R}(\boldsymbol{x}^{(i+1)})) - U(\boldsymbol{R}(\boldsymbol{x}^{(i)}))}{U(\boldsymbol{L}^{(i)}(\boldsymbol{x}^{(i+1)})) - U(\boldsymbol{L}^{(i)}(\boldsymbol{x}^{(i)}))} \tag{6}$$

An implication of the above setup is that the number of EM simulations needed for an iteration with an unaltered updating scheme for the sensitivity matrix is at least $n + 1$. The largest cost driver being the n evaluations required for a full update of $\boldsymbol{J}_R$. In the case of unsuccessful iterations (5) must be re-evaluated with $\boldsymbol{d}$ updated based on the current value of the gain ratio (6), adding an EM simulation for each attempt.

C. EXPEDITED OPTIMIZATION: SENSITIVITY UPDATES USING PRINCIPAL COMPONENTS

In the following two sub-sections, the proposed TR gradient search algorithm involving the principal component analysis (PCA) [38] is formulated. Our procedure utilizes a dedicated updating scheme for the sensitivity matrix, oriented towards the identification of the most relevant directions in the parameter space through PCA.

The most relevant directions are understood here as those the change along which has the most significant effect on the output of the linear model $\boldsymbol{L}^{(i)}$, when averaged over the frequency band of interest.

In our case of a TR gradient search, the initial computation of the sensitivity data is a necessary component of the entire optimization procedure. The gradients described in (4) display the directions and magnitude of change in antenna responses at a specific frequency. We consider the modulus of each gradient as an observable n-dimensional space (n being the number of design variables) that coincides with the original parameter space of the design problem (cf. Fig. 1(a)).

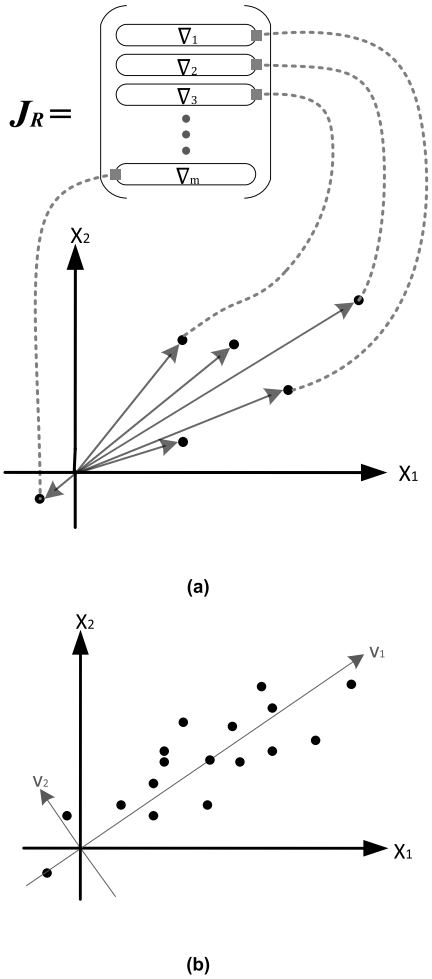

FIGURE 1. Graphical illustration of PCA-based identification of the principal directions determining the largest (frequency-averaged) antenna response variability. (a) Antenna response gradients interpreted as observable vectors. (b) Principal components of the observable set.

In other words, the sensitivity matrix represents a set of directions whose correlations can be identified via PCA.

The means of the gradient moduli are denoted as $\boldsymbol{\mu} = [\mu_1 \ldots \mu_n]^T$. A mean subtracted matrix $\boldsymbol{S} = |\boldsymbol{J}_R| - \boldsymbol{u}\boldsymbol{\mu}^T$ can be created, where $\boldsymbol{u}$ is an $m \times 1$ (unitary) vector of all ones, and $|\boldsymbol{J}_R|$ is a matrix of the gradient moduli (cf. (4)). From this, a covariance matrix is found as [39]

$$\boldsymbol{C} = \frac{1}{m-1}\boldsymbol{S}^T\boldsymbol{S} \tag{7}$$

Note that $\boldsymbol{C}$ is a symmetric square matrix that can be diagonalized as [39]

$$\boldsymbol{C} = \boldsymbol{V}\boldsymbol{E}\boldsymbol{V}^{-1} \tag{8}$$

where $\boldsymbol{V} = [\boldsymbol{v}_1 \ldots \boldsymbol{v}_n]$ is a matrix of eigenvectors and $\boldsymbol{E}$ is a diagonal matrix of the corresponding eigenvalues λ_i, here assumed to be arranged in descending order $\lambda_1 \ge \ldots \ge \lambda_n$. The eigenvectors, here, referred to as principal components, form an orthogonal basis for an n-dimensional ellipsoid, fitted to $\boldsymbol{S}$. The eigenvalues represent the variances of the

observable set projected onto the one-dimensional subspaces spanned by the corresponding eigenvectors. A graphical illustration of these concepts can be found in Fig. 1(b).

The relative variance along the ith eigenvector direction is determined by the normalized eigenvalues

$$\varphi_i = \frac{\lambda_i}{\sum_{k=1}^{n} \lambda_k} \tag{9}$$

The major idea of the accelerated optimization procedure is to limit the finite-differentiation sensitivity updates to the selected principal component directions found through (7)-(9). The rationale being that the main design relocations during the optimization run are to happen along these directions, therefore more precise sensitivity estimation is required therein. For the sake of computational efficiency, we are inclined to use a possibly small number of principal components. The selection is to be governed by their relative importance as determined by the values of φ_i (cf. (9)). By carefully selecting the number of principal components, one can create a low-dimensional representation of directions accountable for the major changes of the antenna outputs.

An additional benefit, transferrable into computational savings, is that relating the sensitivity updates to the principal components allows for an improved generality of the finite-differentiation updates, which can now be realized along arbitrary directions rather than being limited to the coordinate system axes. This restriction also pertains to the accelerated versions of the TR algorithm utilized here as benchmark procedures (cf. Section III.*B*).

D. EXPEDITED OPTIMIZATION: ALGORITHM FLOW

Here, the flow of the proposed algorithm is presented along with a method for incorporating the sensitivity updates with respect to the principal directions (cf. Section II.*C*).

The primary updating scheme, executed upon finding each candidate design using (5), is a rank one Broyden formula [40], where the new Jacobian estimation $\boldsymbol{J}_R^{(i+1)}$ is obtained from the existing one as

$$\boldsymbol{J}_R^{(i+1)} = \boldsymbol{J}_R^{(i)} + \frac{\left(\boldsymbol{f}^{(i+1)} - \boldsymbol{J}_R^{(i)}\boldsymbol{h}^{(i+1)}\right)\boldsymbol{h}^{(i+1)T}}{\boldsymbol{h}^{(i+1)T}\boldsymbol{h}^{(i)}}, \quad i = 0, 1, \ldots \tag{10}$$

where $\boldsymbol{f}^{(i+1)} = \boldsymbol{R}(\boldsymbol{x}^{(i+1)}) - \boldsymbol{R}(\boldsymbol{x}^{(i)})$, and $\boldsymbol{h}^{(i+1)} = \boldsymbol{x}^{(i+1)} - \boldsymbol{x}^{(i)}$. The formula improves the current Jacobian estimate along the direction of $\boldsymbol{h}^{(i+1)}$.

The Broyden formula is also used for incorporating the data acquired by design perturbation along the selected principal components. This is arranged as follows. Let $\boldsymbol{v}_k$ be the principal direction and $\alpha > 0$ be the finite-differentiation step size. Then, the updated Jacobian is obtained using (10) with

$$\boldsymbol{f}^{(i+1)} = \boldsymbol{R}(\boldsymbol{x}^{(i)} + \alpha\boldsymbol{v}_k) - \boldsymbol{R}(\boldsymbol{x}^{(i)}) \quad \text{and } \boldsymbol{h}^{(i+1)} = \alpha\boldsymbol{v}_k \tag{11}$$

The pseudocode provided below describes the basic steps of the proposed algorithm. The following notation is employed:

- K – the number of initial iterations with the Jacobian estimated using complete (i.e., w.r.t. all parameters) finite differentiation;
- N – the number of principal directions used for sensitivity updated thereafter.

The algorithm flow is presented below.

1. Set iteration index $i = 1$;
2. Update the Jacobian matrix
   if $i < \boldsymbol{K}$:
   for $j = 1, \ldots, n$
   Update $\boldsymbol{J}_R^{(i)}$ in the direction x_j via FD;
   end
   else
   Perform PCA where $\boldsymbol{S}$ acts as the input data for (7), (8);
   for $j = 1, \ldots, N$
   Update $\boldsymbol{J}_R^{(i)}$ in the direction $\boldsymbol{v}_j$ (cf. (11));
   end
   end
3. Find the candidate design $\boldsymbol{x}_{tmp}$ by solving (5);
4. Compute ρ and update the TR size using (6);
5. Update $\boldsymbol{J}_R^{(i)}$ in the direction of $\boldsymbol{x}_{tmp} - \boldsymbol{x}^{(i)}$; (cf. (10))
6. ***if*** the termination condition is not satisfied
   set $i = i + 1$ and go to 2;
   else
   END
   end

In Step 2 of the algorithm, the Jacobian is computed either through full finite differentiation (i.e., in the directions of all coordinate system axes), or along the chosen principal components (cf. (11). Further discussion on the selection of the parameters controlling this step, K and N, is provided in the next two paragraphs. In Step 3, the candidate design $\boldsymbol{x}_{tmp}$ is found by solving the subproblem (5) with the objective function $U(\boldsymbol{L}^{(i)}(\boldsymbol{x}))$. In Step 4, the gain ratio ρ is computed, and the trust region size adjusted. In step 5 the Broyden formula (10) is used to update the Jacobian along the direction of the most recent design relocation $\boldsymbol{h}^{(i+1)}$. Figure 2 shows the flow diagram of the entire optimization process.

In the selection of the control parameters K and N, two cost-benefit relationships are considered. Firstly, when increasing the number of initial iterations using complete FD, the cost of gathering sensitivity information increases by n for each iteration (cf. Section II.*B*). The benefit of updating sensitivity information for more than a single iteration becomes clear when considering the scope of change, $\boldsymbol{h}^{(i+1)}$, in the first iterations where the distance to optimum is comparatively large. In the numerical experiments of Section III, $K = 2$ has been chosen as a trade-off between the initial cost of acquiring accurate sensitivity data and computational benefits due to using such data in the subsequent iterations.

Regarding the number N of the principal components used for the Jacobian matrix update, the computational cost of the updates depends linearly on N. On the other hand, adding further components quickly results in diminishing returns

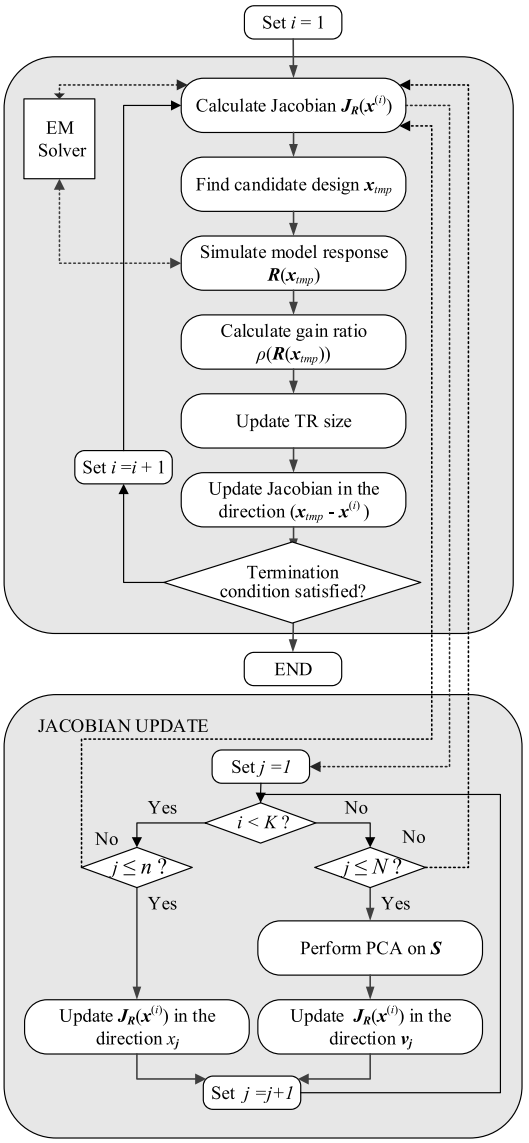

FIGURE 2. Flow diagram of the proposed optimization procedure. Here, N and K are the user-selected parameters controlling the number of principal components employed for sensitivity updates and the number of iterations used for establishing the sensitivity matrix, respectively.

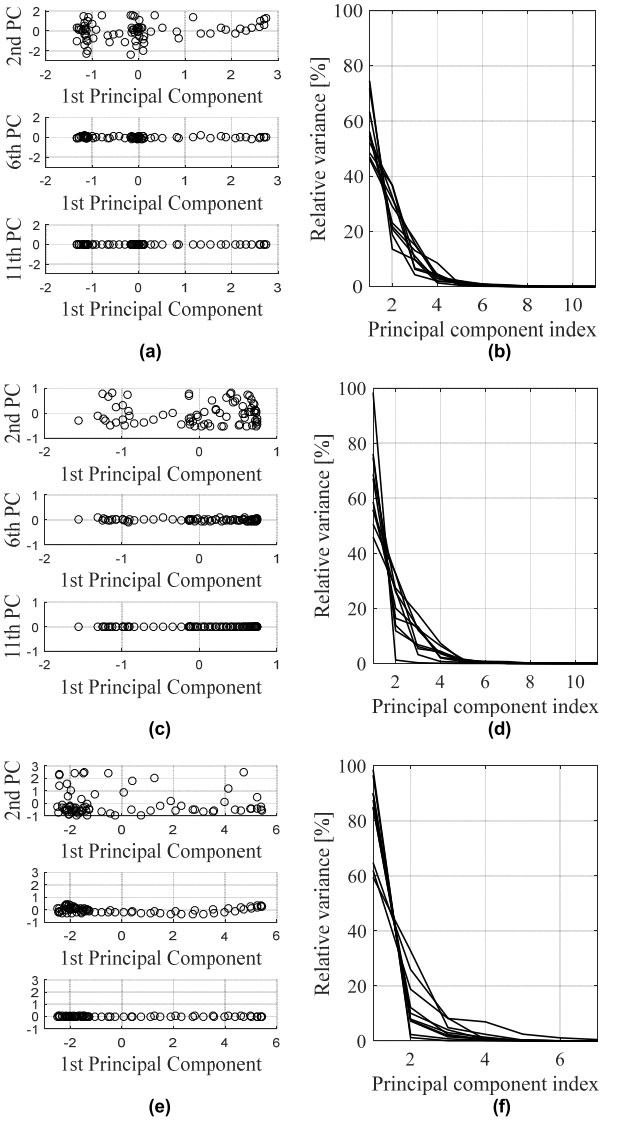

FIGURE 3. Overview of relative variances of antenna response along the principal components. Plots (a)-(b), (c)-(d), and (e)-(f) correspond to Antennas I through III considered in Section III.*A*, respectively. The left-hand-side plots illustrate the variance distribution by principal components, created from sensitivity data of representative initial designs for Antennas I to III. The right-hand-side plots show comparison of the variance explained by principal components; the data extracted from the sensitivity matrices of all initial designs (cf. Section III) for Antennas I through III. Note that the variance levels between the first and the remaining principal components is significant, which justifies utilization of $N = 1$ principal direction in practice.

because the antenna response variability along subsequent principal directions is significantly reduced according to the descending values of the corresponding eigenvalues. As a matter of fact, the difference between the first and the second eigenvalue is already typically large, as can be seen in Fig. 3. Consequently, the $N = 1$ was used in the numerical experiments of Section III.

III. RESULTS

This section provides numerical verification of the proposed optimization algorithm, carried out using the benchmark set of three wideband antennas. The results are compared to the reference TR routine (Section II.*B*) as well as several accelerated versions recently reported in the literature [35]–[37]. Results repeatability is validated by means of the statistical analysis performed for multiple optimization runs executed from random initial designs.

A. CASE STUDIES AND EXPERIMENTAL SETUP

The benchmark set consists of three compact wideband antennas shown in Fig. 4. Antenna I [41] is a standard rectangular monopole featuring a ground plane with L-shape stub for current path enlargement. Its adjustable parameters are $\boldsymbol{x} = [l_0\ g\ a\ l_1\ l_2\ w_1\ o]^T$; with $w_0 = 2o + a$. The feeding line width is set to $w_f = 1.7$ mm to ensure 50 ohm input impedance.

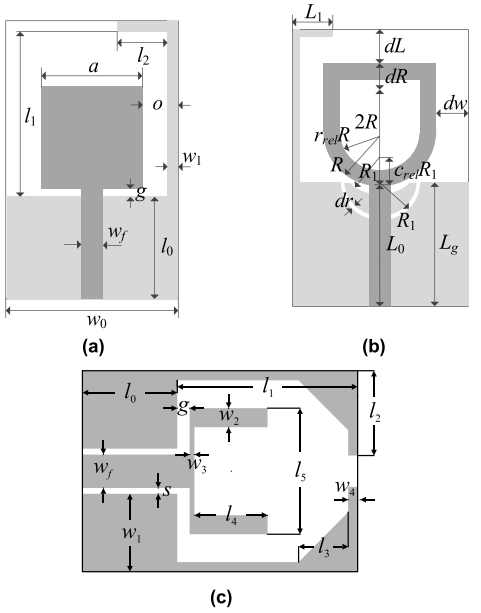

FIGURE 4. Geometries of the benchmark antennas: (a) Antenna I [41], (b) Antenna II [42], (c) Antenna III [43]. For Antennas I and II, the ground plane shown using the light-gray shade.

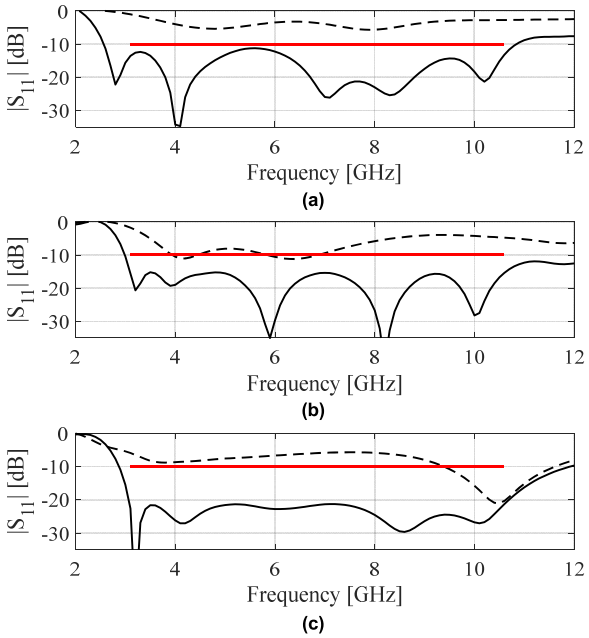

FIGURE 5. Antenna input characteristics for the representative algorithm runs. Horizontal lines indicate the design specifications; (- - -) initial design, (—) optimized design: (a) Antenna I, (b) Antenna II, (c) Antenna III.

Antenna II employs a quasi-circular radiator with a modified ground plane for bandwidth enhancement [42]. The design variables are $\boldsymbol{x} = [L_0\ dR\ R\ r_{rel}\ dL\ dw\ L_g\ L_1\ R_1\ dr\ c_{rel}]^T$.

Antenna III [43] is a uniplanar structure with a driven element in the form of a fork-shaped radiator fed through a coplanar waveguide. Its independent geometry variable vector is $\boldsymbol{x} = [l_0\ l_1\ l_{2r}\ l_{3r}\ l_4\ l_5\ w_1\ w_2\ w_3\ w_4\ g]^T$, with $l_2 = (0.5w_f + s + w_1)\cdot \max\{l_{2r}, l_{3r}\}$ and $l_3 = (0.5w_f + s + w_1)\cdot l_{3r}$; $w_f = 3.5$ and $s = 0.16$ fixed to ensure 50 ohm input impedance.

All structures are implemented on Rogers RO4350 substrate (dielectric permittivity $\varepsilon_r = 3.5$, dielectric loss tan $\delta = 0.0027$, and height $h = 0.76$ mm). The computational models for all structures are implemented in CST Microwave Studio and evaluated using its transient solver. The EM models incorporate SMA connectors.

B. BENCHMARK ALGORITHMS

The benchmark algorithms include the conventional TR-based routine (e.g., [14]), recalled in Section II.*B*, along with the recently reported accelerated versions [35]–[37]. As explained above, the computational overhead of the reference procedure is primarily determined by the cost of the antenna response Jacobian estimation through FD, i.e., n EM additional simulations per each algorithm iteration. The key concept for expediting the basic TR algorithm is to suppress the FD-based gradient updates whenever possible. The latter is decided upon under specific circumstances. The following grounds for omitting FD have been investigated: (i) small relative design change between iterations in particular directions [35], (ii) sufficient alignment between the direction of the most recent design relocation and the coordinate system axes [36], and, (iii) low variability of the response sensitivity throughout the algorithm run [37].

In [35], the omission of FD for the kth parameter depends on the selection factors defined as the relative design relocation (with respect to the TR region size) in the current iteration

$$\varphi_k^i = \left|x_k^{(i+1)} - x_k^{(i)}\right| \Big/ d_k^{(i)}, \quad k = 1, \ldots, n, \tag{12}$$

where $x_k^{(i)}, x_k^{(i+1)}$ refer to the kth components of the parameter vectors $\boldsymbol{x}^{(i)}$, $\boldsymbol{x}^{(i+1)}$ in the last two iterations, respectively; $d_k^{(i)}$ is the kth element of the TR size vector $\boldsymbol{d}^{(i)}$. FD is skipped for the kth parameter if φ_k^i is below a user-defined threshold. Furthermore, the optimization history run is examined in order to ensure that the part of the Jacobian, pertaining to the kth parameter, is estimated through FD at least once every few iterations. The algorithm control parameter is the maximum allowed number of iterations without FD. Increasing it leads to higher potential savings but may compromise the design quality. Typical values range from 3 to 5; more details can be found in [35].

The expedited procedure of [36] replaces, for the selected parameters, FD-based updates by a rank-one Broyden formula (cf. (10)). The decision about skipping FD is based on the alignment factors defined as

$$\gamma_k^{(i)} = \left|\boldsymbol{h}^{(i)T}\boldsymbol{e}^{(k)}\right| \Big/ \left\|\boldsymbol{h}^{(i)}\right\|, \quad k = 1, \ldots, n, \tag{13}$$

where $\boldsymbol{h}^{(i+1)} = \boldsymbol{x}^{(i+1)} - \boldsymbol{x}^{(i)}$, and $\boldsymbol{e}^{(k)}$ refer to the standard basis vectors, i.e., $\boldsymbol{e}^{(k)} = [0 \ldots 010 \ldots 0]^T$ with 1 on the k-th position. For a given parameter, if the alignment factor $\gamma_k^{(i)}$ exceeds a user-specified threshold $0 \le \gamma_{\min} \le 1$ (algorithm control parameter), the appropriate Jacobian portion is updated with the Broyden formula. Increasing $\gamma_{\min}$ imposes a stricter condition for using the Broyden formula and is

TABLE 1. Optimization results for Antenna I.

Algorithm	Cost[#]	Cost savings[##]	max|S_{11}|[$]	Δ max|S_{11}|[$$]	std max|S_{11}|)[*]
Reference	97.6	–	−11.9	–	0.4
This work	36.4	62.7	−12.0	−0.1	0.6
Algorithm of [35]	45.1	53.8	−11.1	0.8	1.1
Algorithm of [37]	31.5	67.7	−11.0	0.9	1.6
Algorithm of [36]	32.3	66.9	−11.4	0.5	1.0

[#] EM simulation count averaged over ten algorithm runs with random initial points.
[##] Relative computational savings in percent w.r.t. the reference algorithm
[$] Maximum $|S_{11}|$ within UWB frequency range (averaged over ten algorithm runs).
[$$] Degradation of max $|S_{11}|$ w.r.t. the reference algorithm in dB.
[*] Standard deviation of maximum of $|S_{11}|$ across the set of 10 algorithm runs.

TABLE 2. Optimization results for Antenna II.

Algorithm	Cost[#]	Cost savings[##]	max|S_{11}|[$]	Δ max|S_{11}|[$$]	std max|S_{11}|)[*]
Reference	111.2	–	−14.9	–	0.6
This work	46.0	58.6	−14.8	0.1	0.6
Algorithm of [35]	58.3	47.6	−13.7	1.2	1.3
Algorithm of [37]	37.5	66.3	−13.9	1.0	1.3
Algorithm of [36]	40.9	63.2	−14.6	0.3	0.9

[#] EM simulation count averaged over ten algorithm runs with random initial points.
[##] Relative computational savings in percent w.r.t. the reference algorithm
[$] Maximum $|S_{11}|$ within UWB frequency range (averaged over ten algorithm runs).
[$$] Degradation of max $|S_{11}|$ w.r.t. the reference algorithm in dB.
[*] Standard deviation of maximum of $|S_{11}|$ across the set of 10 algorithm runs.

advantageous from the point of view of design quality; however, at the cost of reduced computational savings (cf. [36]). Appointing the appropriate value of the alignment threshold is not a trivial task; also, cost-accuracy trade-offs depends on the problem dimensionality.

The last benchmark method [37] involves monitoring of Jacobian variability between consecutive algorithm iterations. This is quantified by the gradient change factor

$$\delta_k^{(i+1)} = \text{std}\left(\frac{\Delta J_k^{(i)}(f)}{M_{J_k^{(i)}(f)}}\right) \tag{14}$$

In (14), the standard deviation is calculated over the frequency range of interest F. The following notation is used: $J_k^{(i)}(f)$ – the k-th column of the Jacobian J_R in the ith iteration of the algorithm, $\Delta J_k^{(i)}(f)$ – the change of the sensitivity w.r.t. the k-th parameter between iterations; $M_{Jk^{(i)}}$ denotes the mean sensitivity for the k-th parameter in subsequent iterations. For a given parameter k, the lower the value of the factor δ_k, the greater the span of iterations, at which FD is suppressed. The algorithm control parameter is the highest number of iterations with FD skipped; typical values vary from 5 to 7. Increasing it results in improved computational efficiency but also a higher potential accuracy loss (cf. [37]).

TABLE 3. Optimization results for Antenna III.

Algorithm	Cost[#]	Cost savings[##]	max|S_{11}|[$]	Δ max|S_{11}|[$$]	std max|S_{11}|)[*]
Reference	96.5	–	−21.7	–	0.9
This work	39.8	58.8	−22.0	−0.3	0.7
Algorithm of [35]	70.9	26.5	−20.9	0.8	3.6
Algorithm of [37]	36.7	62.0	−20.5	1.2	3.5
Algorithm of [36]	41.3	57.2	−21.8	−0.1	1.2

[#] EM simulation count averaged over ten algorithm runs with random initial points.
[##] Relative computational savings in percent w.r.t. the reference algorithm
[$] Maximum $|S_{11}|$ within UWB frequency range (averaged over ten algorithm runs).
[$$] Degradation of max $|S_{11}|$ w.r.t. the reference algorithm in dB.
[*] Standard deviation of maximum of $|S_{11}|$ across the set of 10 algorithm runs.

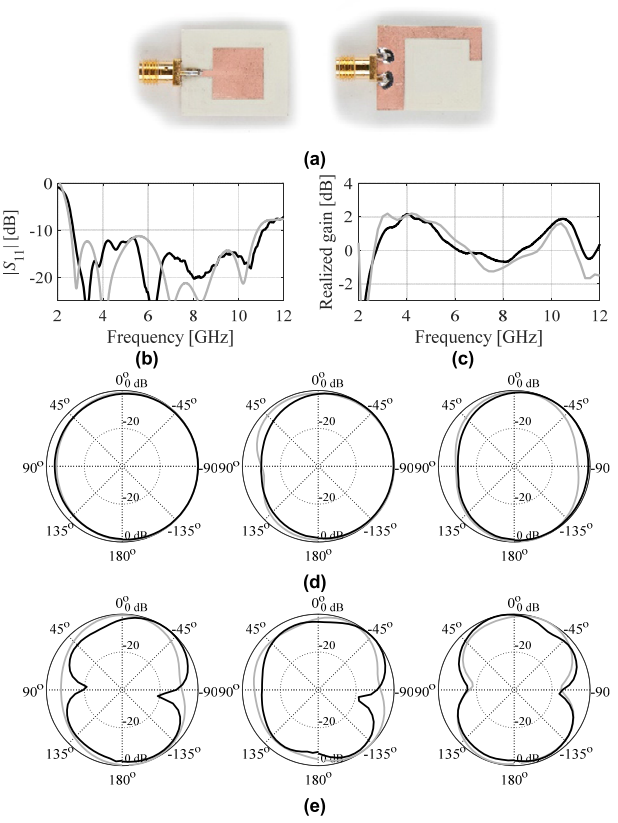

FIGURE 6. Experimental results for Antenna I: (a) photograph of the antenna prototype, (b) reflection responses, (c) realized gain characteristics, (d) H-plane radiation patterns (from left to right: 4 GHz, 6 GHz, 8 GHz), (e) E-plane radiation patterns (from left to right: 4 GHz, 6 GHz, 8 GHz). Simulations and measurements shown as gray and black curves, respectively.

C. NUMERICAL RESULTS AND DISCUSSION

The benchmark antennas (cf. Section III.*A*) have been optimized for best in-band matching within the UWB frequency range from 3.1 GHz to 10.6 GHz. The detailed description of the optimization task has been provided in Section II.*A*. Multiple algorithm runs have been executed using random initial designs in order to verify reliability of the

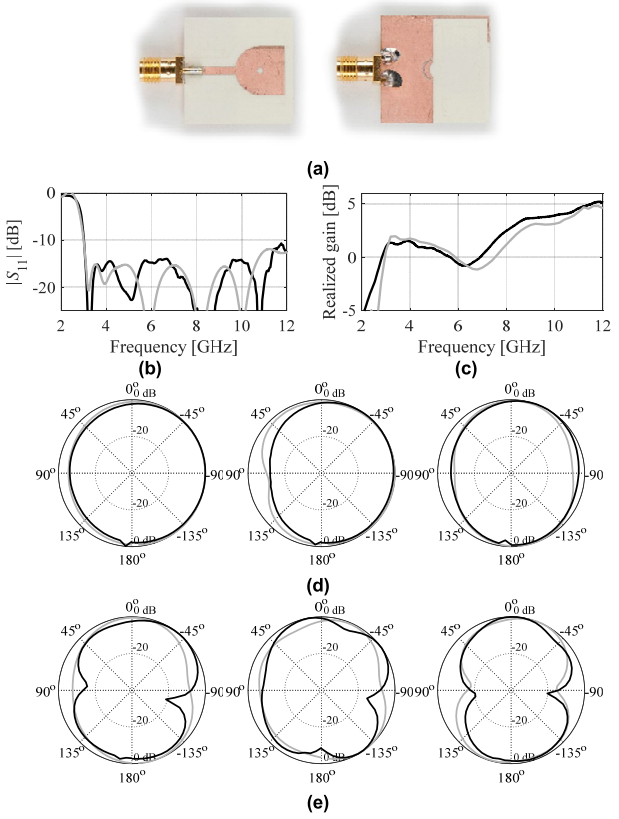

FIGURE 7. Experimental results for Antenna II: (a) photograph of the antenna prototype, (b) reflection responses, (c) realized gain characteristics, (d) H-plane radiation patterns (from left to right: 4 GHz, 6 GHz, 8 GHz), (e) E-plane radiation patterns (from left to right: 4 GHz, 6 GHz, 8 GHz). Simulations and measurements shown as gray and black curves, respectively.

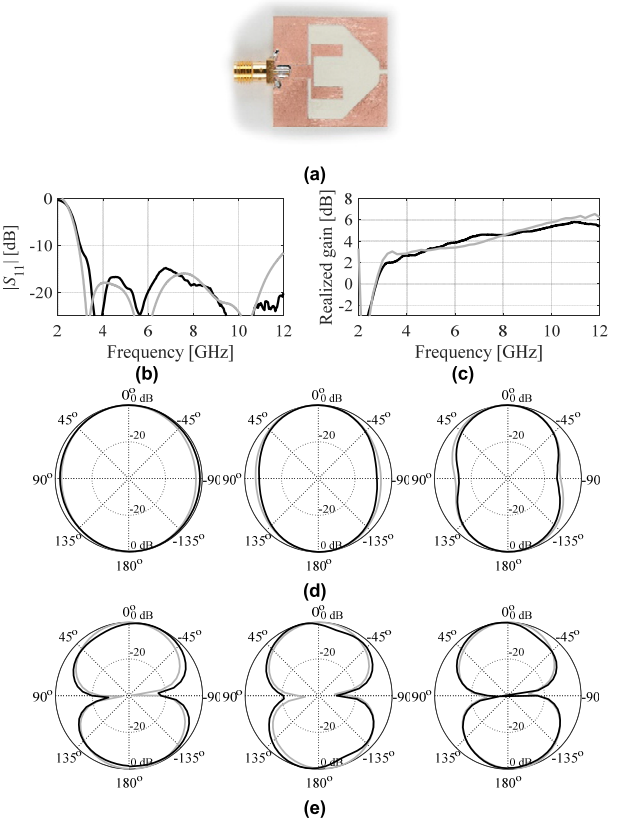

FIGURE 8. Experimental results for Antenna III: (a) photograph of the antenna prototype, (b) reflection responses, (c) realized gain characteristics, (d) H-plane radiation patterns (from left to right: 4 GHz, 6 GHz, 8 GHz), (e) E-plane radiation patterns (from left to right: 4 GHz, 6 GHz, 8 GHz). Simulations and measurements shown as gray and black curves, respectively.

optimization process. The results are compared with those obtained using the reference algorithm (cf. Section II.*B*) and the accelerated procedures (cf. Section III.*B*).

Tables 1 through 3 gather the numerical data. It should be noted that the standard deviation of the objective function (the last column in the tables) is larger than zero even for the reference algorithm because different initial designs generally lead to slightly different local optima. This is a result of parameter redundancy in the antenna structures but also certain level of numerical noise in EM simulation results, which does not permit the gradient-based procedures to perfectly allocate the optimum. An evaluation of the algorithm robustness should thus be conducted in a relative sense, i.e., by a comparison with the reference algorithm quality indicators. Antenna responses for the representative algorithm runs have been shown in Fig. 5.

It can be observed that the proposed algorithm performs consistently over the considered benchmark set. The design quality demonstrated is on par or, in the case of Antenna III, even better than the reference algorithm. This is the case for both the average objective function values but also the standard deviation, which is equal to that of the reference procedure and lower than that of all the benchmark algorithms. This confirms the reliability of the routine. High design quality is achieved while delivering computational savings of about sixty percent, on the average. In some cases, the algorithms of [37] and [36] deliver higher savings than the proposed procedure, yet, at a price of the design quality degradation and worsened result repeatability. The quality of designs yielded by the benchmark algorithms [35]–[37] is similar and noticeably lower than for the method proposed in this paper.

D. EXPERIMENTAL VALIDATION

The selected optimized designs of Antennas I through III have been fabricated and measured for additional validation. Figures 6 through 8 show the photographs of the antenna prototypes as well as the comparison of the simulated and measured results. The agreement between both data sets is good. Slight misalignments result from manufacturing and assembly inaccuracies as well as the experimental setup, particularly in the case of E-plane patterns, where a 90-degree bend (not included in the computational model) has been used to mount the structures.

IV. CONCLUSION

The paper proposed a procedure for expedited gradient-based design optimization of antenna structures using numerical derivatives. The foundation of the method is the sparse sensitivity updating scheme, which is conducted along the selected principal directions, determining the maximum variability of the antenna characteristics, averaged over the frequency range of interest. This is supplemented by the Jacobian matrix enhancement through the rank-one Broyden formula using EM simulation of the candidate designs rendered during each iteration of the optimization process.

The comprehensive numerical verification of the proposed procedure indicates that significant (up to almost 60 percent) computational savings can be achieved with respect to the reference algorithm employing full finite-differentiation Jacobian updates in each iteration. At the same time, these benefits are obtained without compromising the design quality, which is similar or even better—for certain test problems—than that of the reference algorithm.

This was not the case for the previously reported accelerated algorithms, here, utilized as the benchmark. Although some exhibit slightly better computational efficiency, their speedup comes at the expense of quality degradation, sometimes rather significant. All benchmark procedures are based on suppressing the sensitivity updates for particular antenna parameters meaning that incorporation of the new EM data is always restricted to the coordinate system axes. As opposed to that, the updating direction for the proposed method can, in principle, be arbitrary. This seems to be one of the important factors behind the efficacy of the framework.

The presented approach may be useful to speed up direct optimization of EM antenna models. It can also be applied within variable-fidelity design framework, e.g., for solving optimization sub-problems at the low-fidelity simulation level.

ACKNOWLEDGMENT

The authors would like to thank Dassault Systemes, France, for making CST Microwave Studio available.

REFERENCES

[1] M. K. Ray, K. Mandal, and N. Nasimuddin, "Low-profile circularly polarized patch antenna with wide 3 dB beamwidth," *IEEE Antennas Wireless Propag. Lett.*, vol. 18, no. 12, pp. 2473–2477, Dec. 2019, doi: 10.1109/lawp.2019.2940703.
[2] W.-H. Ng, E.-H. Lim, F.-L. Bong, and B.-K. Chung, "E-shaped folded-patch antenna with multiple tuning parameters for on-metal UHF RFID tag," *IEEE Trans. Antennas Propag.*, vol. 67, no. 1, pp. 56–64, Jan. 2019.
[3] B. Peng, S. Li, J. Zhu, L. Deng, and Y. Gao, "A compact wideband dual-polarized slot antenna with five resonances," *IEEE Antennas Wireless Propag. Lett.*, vol. 16, pp. 2366–2369, 2017.
[4] D. Xie and L. Zhu, "Effective approach to reduce variation of quasi-E-plane beamwidth of EH1-mode microstrip leaky-wave antennas," *IEEE Antennas Wireless Propag. Lett.*, vol. 17, no. 9, pp. 1732–1735, Sep. 2018.
[5] J.-L. Liu, T. Su, and Z.-X. Liu, "High-gain grating antenna with surface wave launcher array," *IEEE Antennas Wireless Propag. Lett.*, vol. 17, no. 4, pp. 706–709, Apr. 2018.
[6] S. Lei, Y. Yang, H. Hu, Z. Zhao, B. Chen, and X. Qiu, "Power gain optimization method for wide-beam array antenna via convex optimization," *IEEE Trans. Antennas Propag.*, vol. 67, no. 3, pp. 1620–1629, Mar. 2019.
[7] A. A. Deshmukh, P. Verma, and S. Pawar, "Variations of P-shape microstrip antennas for multi-band dual polarised response," *IET Microw., Antennas Propag.*, vol. 13, no. 3, pp. 398–405, Feb. 2019.
[8] Y. Xu, J. Wang, L. Ge, X. Wang, and W. Wu, "Design of a notched-band Vivaldi antenna with high selectivity," *IEEE Antennas Wireless Propag. Lett.*, vol. 17, no. 1, pp. 62–65, Jan. 2018.
[9] S. Kim and S. Nam, "A compact and wideband linear array antenna with low mutual coupling," *IEEE Trans. Antennas Propag.*, vol. 67, no. 8, pp. 5695–5699, Aug. 2019.
[10] W. Li, Y. Wang, B. You, Z. Shi, and Q. H. Liu, "Compact ring slot antenna with harmonic suppression," *IEEE Antennas Wireless Propag. Lett.*, vol. 17, no. 12, pp. 2459–2463, Dec. 2018.
[11] A. M. Alzahed, S. M. Mikki, and Y. M. M. Antar, "Nonlinear mutual coupling compensation operator design using a novel electromagnetic machine learning paradigm," *IEEE Antennas Wireless Propag. Lett.* , vol. 18, no. 5, pp. 861–865, May 2019.
[12] L. Liu, S. W. Cheung, and T. I. Yuk, "Compact MIMO antenna for portable UWB applications with band-notched characteristic," *IEEE Trans. Antennas Propag.*, vol. 63, no. 5, pp. 1917–1924, May 2015.
[13] U. Ullah and S. Koziel, "A geometrically simple compact wideband circularly polarized antenna," *IEEE Antennas Wireless Propag. Lett.* , vol. 18, no. 6, pp. 1179–1183, Jun. 2019.
[14] J. Nocedal and S. Wright, *Numerical Optimization*, 2nd ed. New York, NY, USA: Springer, 2006.
[15] D. Guirguis and M. F. Aly, "A derivative-free level-set method for topology optimization," *Finite Elements Anal. Des.*, vol. 120, pp. 41–56, Nov. 2016.
[16] E. N. Tziris, P. I. Lazaridis, Z. D. Zaharis, J. P. Cosmas, K. K. Mistry, and I. A. Glover, "Optimized planar elliptical dipole antenna for UWB EMC applications," *IEEE Trans. Electromagn. Compat.*, vol. 61, no. 4, pp. 1377–1384, Aug. 2019.
[17] A. Lalbakhsh, M. U. Afzal, and K. P. Esselle, "Multiobjective particle swarm optimization to design a time-delay equalizer metasurface for an electromagnetic band-gap resonator antenna," *IEEE Antennas Wireless Propag. Lett.*, vol. 16, pp. 912–915, 2017.
[18] S. K. Goudos, K. Siakavara, T. Samaras, E. E. Vafiadis, and J. N. Sahalos, "Self-adaptive differential evolution applied to real-valued antenna and microwave design problems," *IEEE Trans. Antennas Propag.*, vol. 59, no. 4, pp. 1286–1298, Apr. 2011.
[19] R.-Q. Wang and Y.-C. Jiao, "Synthesis of wideband rotationally symmetric sparse circular arrays with multiple constraints," *IEEE Antennas Wireless Propag. Lett.*, vol. 18, no. 5, pp. 821–825, May 2019.
[20] J. Zhang, C. Zhang, F. Feng, W. Zhang, J. Ma, and Q.-J. Zhang, "Polynomial chaos-based approach to yield-driven EM optimization," *IEEE Trans. Microw. Theory Techn.*, vol. 66, no. 7, pp. 3186–3199, Jul. 2018.
[21] A. Kouassi, N. Nguyen-Trong, T. Kaufmann, S. Lallechere, P. Bonnet, and C. Fumeaux, "Reliability-aware optimization of a wideband antenna," *IEEE Trans. Antennas Propag.*, vol. 64, no. 2, pp. 450–460, Feb. 2016.
[22] J. Wang, X.-S. Yang, and B.-Z. Wang, "Efficient gradient-based optimisation of pixel antenna with large-scale connections," *IET Microw., Antennas Propag.*, vol. 12, no. 3, pp. 385–389, Feb. 2018.
[23] E. Hassan, D. Noreland, R. Augustine, E. Wadbro, and M. Berggren, "Topology optimization of planar antennas for wideband near-field coupling," *IEEE Trans. Antennas Propag.*, vol. 63, no. 9, pp. 4208–4213, Sep. 2015.
[24] *CST Microwave Studio*, CST AG, Darmstadt, Germany, 2018.
[25] S. Koziel and S. Ogurtsov, *Antenna Design by Simulation-Driven Optimization. Surrogate-Based Approach*. New York, NY, USA: Springer, 2014.
[26] S. Koziel and A. Bekasiewicz, *Multi-Objective Design of Antennas Using Surrogate Models*. Cleveland, OH, USA: World, 2016.
[27] J. Gong, F. Gillon, J. T. Canh, and Y. Xu, "Proposal of a kriging output space mapping technique for electromagnetic design optimization," *IEEE Trans. Magn.*, vol. 53, no. 6, pp. 1–4, Jun. 2017.
[28] J. P. Jacobs, "Characterisation by Gaussian processes of finite substrate size effects on gain patterns of microstrip antennas," *IET Microw., Antennas Propag.*, vol. 10, no. 11, pp. 1189–1195, Aug. 2016.
[29] J. Xu, M. Li, and R. Chen, "Space mapping optimisation of 2D array elements arrangement to reduce the radar cross-scattering," *IET Microw., Antennas Propag.*, vol. 11, no. 11, pp. 1578–1582, 2017.
[30] S. Koziel and L. Leifsson, *Simulation-Driven Design by Knowledge-Based Response Correction Techniques*. New York, NY, USA: Springer, 2016.
[31] S. Koziel and S. D. Unnsteinsson, "Expedited design closure of antennas by means of trust-region-based adaptive response scaling," *IEEE Antennas Wireless Propag. Lett.*, vol. 17, no. 6, pp. 1099–1103, Jun. 2018.

[32] S. Koziel, "Fast simulation-driven antenna design using response-feature surrogates," *Int. J. RF Microw. Comput.-Aided Eng.*, vol. 25, no. 5, pp. 394–402, Jun. 2015.
[33] M. Diez, S. Volpi, A. Serani, F. Stern, and E. F. Campana, "Simulation-based design optimization by sequential multi-criterion adaptive sampling and dynamic radial basis functions," in *Advances in Evolutionary and Deterministic Methods for Design, Optimization and Control in Engineering and Sciences* (Computational Methods in Applied Sciences), vol. 48, E. Minisci, M. Vasile, J. Periaux, N. Gauger, K. Giannakoglou, and D. Quagliarella, Eds. Cham, Switzerland: Springer, 2019.
[34] S. Koziel and A. Bekasiewicz, "Reliable low-cost surrogate modeling and design optimisation of antennas using implicit space mapping with substrate segmentation," *IET Microw., Antennas Propag.*, vol. 11, no. 14, pp. 2066–2070, Nov. 2017.
[35] S. Koziel and A. Pietrenko-Dabrowska, "Reduced-cost electromagnetic-driven optimisation of antenna structures by means of trust-region gradient-search with sparse Jacobian updates," *IET Microw., Antennas Propag.*, vol. 13, no. 10, pp. 1646–1652, Aug. 2019.
[36] S. Koziel and A. Pietrenko-Dabrowska, "Expedited optimization of antenna input characteristics with adaptive Broyden updates," *Eng. Comput.*, to be published, doi: 10.1108/ec-01-2019-0023.
[37] A. Pietrenko-Dabrowska and S. Koziel, "Computationally-efficient design optimization of antennas by accelerated gradient search with sensitivity and design change monitoring," *IET Microw., Antennas Propag.*, to be published, doi: 10.1049/iet-map.2019.0358.
[38] I. T. Jolliffe, *Principal Component Analysis*, 2nd ed. New York, NY, USA: Springer, 2002.
[39] C. M. Bishop, *Pattern Recognition and Machine Learning*. New York, NY, USA: Springer, 2006.
[40] C. G. Broyden, "A class of methods for solving nonlinear simultaneous equations," *Math. Comp.*, vol. 19, no. 92, p. 577, 1965.
[41] M. A. Haq, S. Koziel, and Q. S. Cheng, "EM-driven size reduction of UWB antennas with ground plane modifications," in *Proc. Int. Appl. Comp. Electromagn. Soc. (ACES China) Symp.*, 2017.
[42] M. G. N. Alsath and M. Kanagasabai, "Compact UWB monopole antenna for automotive communications," *IEEE Trans. Antennas Propag.*, vol. 63, no. 9, pp. 4204–4208, Sep. 2015.
[43] X. Qing and Z. Chen, "Compact coplanar waveguide-fed ultra-wideband monopole-like slot antenna," *IET Microw. Antennas Propag.*, vol. 3, no. 5, pp. 889–898, 2009.

JON ATLI TOMASSON is currently pursuing the B.Sc. degree in mechatronic engineering with the Department of Engineering, Reykjavik University, Iceland. His research interests include simulation-driven design, surrogate-based optimization, evolutionary computation, dynamical systems, and stochastic processes.

SLAWOMIR KOZIEL received the M.Sc. and Ph.D. degrees in electronic engineering from the Gdansk University of Technology, Poland, in 1995 and 2000, respectively, the M.Sc. degrees in theoretical physics and in mathematics, in 2000 and 2002, respectively, and the Ph.D. degree in mathematics from the University of Gdansk, Poland, in 2003. He is currently a Professor with the Department of Engineering, Reykjavik University, Iceland. His research interests include CAD and modeling of microwave and antenna structures, simulation-driven design, surrogate-based optimization, space mapping, circuit theory, analog signal processing, evolutionary computation, and numerical analysis.

ANNA PIETRENKO-DABROWSKA received the M.Sc. and Ph.D. degrees in electronic engineering from the Gdansk University of Technology, Poland, in 1998 and 2007, respectively. She is currently an Associate Professor with the Gdansk University of Technology. Her research interests include simulation-driven design, design optimization, control theory, modeling of microwave and antenna structures, as well as numerical analysis.